[1]Naturally Fractured Gas Reservoirs Detection Optimization: Wind River Basin

David R. Phillips, dave@ mail.geometrics.com, (303)278-8700
Robert E. Grimm, grimm@mail.blackhawkgeo.com, (303)278-8700
Blackhawk Geometrics, Inc.
301 Commercial Road, Suite B
Golden, CO 80401

Heloise B. Lynn, 75122,3652@compuserve.com, (713)556-9196
K. Michele Simon,
Lynn Incorporated
1646 Fall Valley Dr.
Houston, TX 77077

Introduction

Many gas fields in the Rocky Mountain region produce from natural fractures, and the orientation and concentration of these natural fractures are often the most significant factors controlling gas production. The primary research goal of this project is the detection of gas filled fractures using surface seismic P-wave methods. If highly fractured areas can be located using seismic techniques prior to drilling, it can greatly benefit the field development of the reservoirs.

This project is in the third year of a three year contract. The study area is a gas field in Wyoming's Wind River Basin. The target is the Lower Fort Union formation (LFU), at 5,000-10,000 ft (1.6-3.0 km) depth, a non-marine sequence of thin layers of shales, silts, sands, and a few thin coal units. Commercial production rates are incommensurate with matrix permeability and matrix porosities. Fracture density is known to be a dominant factor in well productivity. Matrix porosities range from 2-7% (which are not perceived to contribute significantly to commerciality) to occasionally 8-16% (which if present will contribute to commerciality). Matrix permeability from repeat formation tester data in four wells range from 0.5 md to 10 md, in the LFU formation, with 3-5 md being the median matrix permeability.

The physical phenomenon that we are exploiting is azimuthal anisotropy. Vertical aligned gas-filled fractures function as additional ordered compliant members in a host or matrix rock. The presence of additional ordered compliant members causes azimuthal anisotropy; that is, the properties of seismic wave propagation (velocity, amplitude, frequency content,

[1] Research sponsored by the U.S. Department of Energy's Federal Energy Technology Center, under contract DE-AC21-94MC31224 with Blackhawk Geometrics, 301 Commercial Road, Suite B, Golden, CO 80401 Fax: (303) 278 0789

attenuation, etc.) depend upon the azimuth of the source-receiver raypath. Our task is to acquire, process, and interpret 3D P-wave multiazimuth data in a manner that records and highlights the azimuth dependency of various measurements, so that a comparison with EUR (estimated ultimate recovery) can be made. After a correlation with EUR is made, maps showing the presence of the well-correlated seismic attributes are prepared.

Approach

Wide-azimuth (source-receiver, S-R) 3D P-wave data were acquired over 37 square miles (95 square km) by our industry partner. The acquisition parameters included circular geophone arrays and single-hole dynamite charges, so that this study could have azimuthally isotropic sources and receivers.

The important azimuths in the LFU were tabulated. We documented the dominant azimuths of maximum horizontal present-day stress, as interpreted from borehole elongation, and the dominant azimuths of fractures seen in cores and borehole image logs. A preponderance of east-west (EW) azimuths is observed in these data, although some scatter exists. The dominant fault azimuth mapped in the 3D-processed data was N100E ($\pm$5), as shown in Figure 1, a time structure map at the top of the Lower Fort Union level.

The orientation of the P-wave seismic anisotropy was determined by creating supergathers (bin size 600m by 600m) and with primary sort by azimuth and secondary sort by offset (10 degree slices, from 0^o to 180^o, that is, 18 gathers, with offsets from 15-3050 m). The analysis of nine azimuth-supergathers established that the seismic velocity anisotropy is oriented EW / NS; the data provided the clear direction to divide the EW source-receiver azimuths ($\pm$45 degrees) from the NS source-receiver azimuths ($\pm$45 degrees). Subsequently, we formed two volumes:

1. Source-receiver azimuth parallel to the minimum traveltime direction (fast velocity direction) which is EW, $\pm$45 degrees;
2. Source-receiver azimuth parallel to the maximum traveltime direction (slow velocity direction) which is North-South, $\pm$45 degrees.

Examples of supergathers from this project are found in Lynn et al., “Fracture detection, mapping, and analysis of naturally fractured gas reservoirs using seismic technology”, presented at this conference.

Each limited azimuth volume was then processed independently through pre-stack time migration. Migrated gathers were needed for AVO analysis by azimuth which would directly tie the maps made on the pre-stack time-migrated data. Each volume had velocities picked independently on pre-stack time migrated gathers.

Confirmation of the fast P-wave velocity direction was seen in the shear wave arrivals in the 9C VSP: the fast shear wave (S1) azimuth in the LFU of N110E was observed from 1.6 km

(5300 ft) to 2.2 km (7300 ft). Anomalies of 8 -12% S-wave velocity anisotropy were seen in crossed-dipole S-wave sonic and in the VSP data

Analysis

Transmission anomalies and reflection anomalies were examined. Transmission anomalies include: interval velocity differences by azimuth; average interval frequency differences by azimuth. The interval velocity was calculated using the Dix equation for the top 300 msec (approx. 1500 ft (450 m)) of the LFU. Figure 2 shows the ratio of interval velocities for the top 300 ms of the LFU, taken as (Int. Vel. NS)/(Int. Vel. EW).

Reflection anomalies that were analyzed at the top LFU reflector include: reflection strength difference by azimuth; reflector AVO gradient difference by azimuth.

Estimated ultimate recovery (EUR) from the LFU was provided by our industry partner in 19 control wells: 12 commercially productive wells and 7 low- to non-productive wells. The five seismic attributes evaluated relative to EUR were: the ratio of interval velocity (NS/EW) in the top 1500 ft of LFU, the difference in interval frequency content (NS-EW) in the top 1500 ft of LFU, the sum of the AVO gradients (NS + EW) at the top LFU reflector, the difference of the AVO gradients (NS-EW) at the top LFU reflector, and the difference of the reflection strength (NS-EW) for the top LFU reflector. The azimuthal attribute that correlated best with commercial production was the ratio of the interval velocity: 10 out of the 12 desirable EUR wells showed between 0.85-0.95 as the value of the ratio NS interval velocity/EW interval velocity, with median value of 0.91 (Figure 3).

In the preliminary analysis, an attribute was considered “prospective” if it was associated with most of the wells with high gas production (EUR >8.0 BCF), in our control set of wells (Figure 4).

The correlation of “prospective” seismic attributes with the twelve high-production wells, is shown in Figure 5. This technique is useful for identifying good locations, not for condemning bad locations (Figure 6).

Figure 7 shows the overlay of the presence of the five prospective attributes, for a portion of the survey. The time structure map of the top LFU is shown in relief, and the colors are the weighted value of the “prospective”, or positive, seismic attributes. Of the five positive seismic attributes, all but the velocity anisotropy were given a weight of 1. The velocity anisotropy was assigned a weight of 5. Therefore, values of 6, 7, 8 and 9 show where the velocity anisotropy plus other positive attributes are present.

Modeling and Analysis of AVO (amplitude variation with offset)

Amplitudes are more sensitive than travel times to experiment and environment, being significantly influenced by source strength, source and receiver coupling and directivity, spherical divergence, absorption, scattering and multiples, transmission and reflection coefficients and their variation with incidence angle, anisotropy, and reflector curvature and rugosity (Sheriff, 1975). As there is both significant anisotropy and reflector structure in the units of interest in the Wind River Basin, it is prudent to evaluate the magnitudes of these effects on measured AVO indicators of fracturing and/or gas concentration.

The approach is to compute synthetic seismograms using the actual 37mi^2 survey geometry and seismic structure derived from this experiment. AVO was parameterized using the standard model $R = a + b \sin^2\theta$ and was separated into NS and EW azimuths. As a preliminary test, flat isotropic layers were modeled using the real survey geometry. Apparent differences or biases of up to a few tens of percent in AVO gradient *b* between NS and EW azimuths were present in this test purely due to the survey layout: the NS line orientations or elongated receiver patches lead to more long-offset sampling in this direction and therefore AVO fits are weighted differently in long and short directions. Because $R = a + b \sin^2\theta$ is an imperfect model, with an error varying systematically with incidence angle (offset), the two azimuths show different AVO, with magnitudes smaller in the long direction.

Complex structure scatters seismic energy, broadening the amplitude response at any incidence angle. This greater scatter in the AVO data lowers the estimated magnitudes of *a* and *b*. Anisotropy has profound effects on the sign and magnitude of AVO gradient: for a positive impedance contrast, layering anisotropy above the reflector (isotropic below) results in large negative *b*, whereas vertical-crack anisotropy below the reflector (isotropic above) causes weakly negative or slightly positive gradients. These variations can be understood in terms of the change in Poisson's ratio σ as a function of incidence angle for fluid-filled cracks: σ increases for raypaths in the slow (crack-perpendicular) direction. Therefore an overlying layering anisotropy will have a higher σ in this upper layer at near offsets, whereas an underlying vertical-crack anisotropy will have a higher in the lower layer at far offsets. Ostrander (1984) showed that a decrease in σ across an interface is accompanied by a negative AVO gradient, whereas a positive change in σ results in positive b. These cases correspond to the overlying layering anisotropy and underlying vertical anisotropy, respectively. Because the near-offset response is larger than that at far offsets, the
effect of overlying layering anisotropy dominates when combined with underlying vertical anisotropy, yielding a relatively large negative AVO gradient.

Although significant effects of structure and anisotropy are evident, the azimuthal differences in these models are still comparatively modest, averaging several tens of

percent. However, individual bins can nonetheless show azimuthal variations up to a few hundred percent; these locations must then be identified as potential sites in the actual AVOA data that are strongly influenced by survey geometry, structure, and/or anisotropy and should be interpreted with caution. To date we have found no serious discrepancies with the data; ongoing effort includes subtraction of the best structure / anisotropy model from the AVOA data to test for improved correlation with gas pay.

Results To Date

The search for areas of high fracture density in a naturally fractured gas reservoir is accomplished by searching for areas of additional ordered compliance. In this Wind River project, rocks that appear (seismically) more compliant in the NS azimuth but stiffer in the orthogonal azimuth (EW) are interpreted to contain EW-trending gas-filled vertical aligned fractures. From previous work, it has been established that the greater the magnitude of the shear wave seismic anisotropy, the greater the magnitude of the fracture density (Crampin, 1985). Lynn et al. (1996) showed that the difference in the P-wave AVO gradient by azimuth is proportional to the magnitude of the shear wave anisotropy. Presented here is the 3D, P-wave extension of prior 2D evaluations of seismic anisotropy using multicomponent field data (9C reflection seismic and VSP).

The differences by azimuth (NS-EW or NS/EW) in various seismic quantities as extracted from two 3D pre-stack time-migrated volumes (acquired at the same time in the field) are possible indications of P-wave seismic anisotropy. Since different raypaths are involved, the question of heterogeneity (different rocks) or anisotropy arises, which is the focus of our future work.

Further Work

A 2 sq. mi. (5.2 sq. km) 3D-3C survey acquired two years ago in the center of this 37 sq. mi. (95 sq. km) survey will provide P-P and P-S events that will help evaluate the relationship of P-wave azimuthal anisotropy to S-wave traveltime anisotropy, and hence the fracture density. The S-wave polarizations will tell us about the stiff direction in the rock in the last medium traversed. Layer-stripping and 4-component rotation algorithms applied to P-S data may help in evaluating the anisotropy present and its manifestations on P-wave multi-azimuth data.

Benefits

The use of P-waves to detect azimuthal anisotropy represents a significant cost benefit when compared to the traditional use of shear waves for this purpose. We foresee reductions in the acquisition cost of multi-azimuth P-wave surveys (as larger and larger recording channel systems become available), since only conventional seismic sources and receivers are required. Since some shear wave data are desirable for calibration of the P-wave data, acquisition of a multi-component VSP or a small patch of converted-wave

(3C) data is recommended. As successful identification of high fracture density zones can be made with 3-D multi-azimuth P-wave data plus small quantities of shear wave data, this technology will have broad appeal to operators in tight gas plays in the Rocky Mountain basins, as well as other areas.

Acknowledgements

This work was funded by the U.S. Dept. of Energy, Federal Energy Technology Center, under contract DE-AC21-94MC31224, Naturally Fractured Tight Gas Reservoir Detection, with Blackhawk Geometrics, 301 Commercial Rd., Ste., B, Golden, CO 80401, fax (303) 278 0789.. We thank Bill Gwilliam and Royal Watts (retired) of US DOE Federal Energy Technology Center, Morgantown, WV for their leadership and input on this work. We gratefully acknowledge our Industry Partner, the owner/operator in the field in which this data was collected, for their contribution of production data, geologic data, and field historical development information. This project is the 3D extension of 2D seismic field data techniques demonstrated in the FETC/DOE project no. DE-AC21-2MC28135 at Bluebell-Altamont, Utah.

References

Crampin, S., 1985, Evaluation of anisotropy by shear-wave splitting, Geophysics, vol. 50, no. 1, 142-152.

Johnson, W., 1995, Direct detection of gas in pre-Tertiary sediments?, The Leading Edge, vol. 14,
119-122.

Lynn, H.B., Simon, K.M., Bates, C.R., and Van Dok, R., 1996, Azimuthal anisotropy in P-wave 3-D (multiazimuth) data, The Leading Edge, vol. 15, no. 8, 923-928.

MacBeth, C., 1996, Edinburgh Anisotropy Project, British Geological Survey, West Mains Road,
Murchison House, Edinburgh, Scotland EH9 3LA. http://www.gsrg.nmh.ac.uk/

Ostrander, W.J., 1984, Plain waves reflection coefficients for gas sands at non-normal angles of incidence, Geophysics, vol. 49, 1637-1648

Sheriff, R., 1975, Factors affecting seismic amplitude, Geophys. Prosp, vol. 23, 125-138

Figure Captions

Figure 1. Time structure map on top LFU formation. Faults interpreted from the 3D data strike approximately N100E.

Figure 2. Ratio of interval velocities in the top 300 ms (450 m) of the Lower Fort Union. Warm colors indicate faster velocities EW than NS; cool colors indicate faster velocities NS than EW.

Figure 3. Interval velocity ratio in top 300 ms of LFU plotted versus well rank. Most of the top-ranked wells show significant velocity anisotropy (NS/EW less than 0.95)

Figure 4. Success rate of the seismic attributes evaluated in the Wind River study. Of the attributes evaluated, interval velocity ratio shows the best correlation with gas production.

Figure 5. Seismic attributes observed at the twelve best producing wells, gives an indication of how well the seismic attributes predict gas production.

Figure 6. Seismic attributes observed at the seven poorly-ranked wells shows that the seismic attributes do not effectively predict non-production.

Figure 7. Time structure map of top LFU shown in relief with multiple positive seismic attributes overlain in color. Positive seismic attributes are assigned a weight of 1 with the exception of interval velocity ratio, assigned a weight of 5.

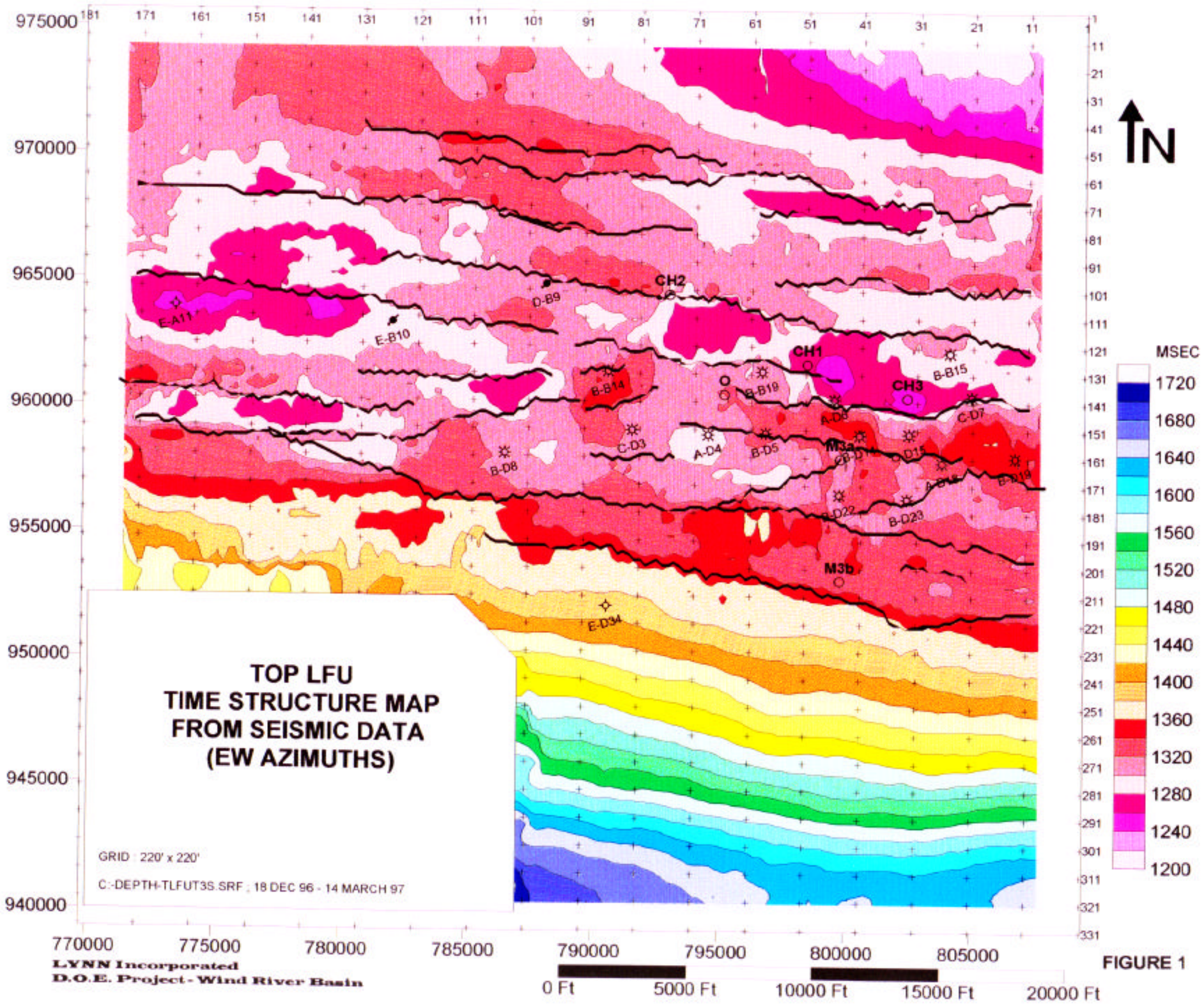
TOP LFU
TIME STRUCTURE MAP
FROM SEISMIC DATA
(EW AZIMUTHS)
GRID : 220' x 220'
C:-DEPTH-TLFUT3S.SRF ; 18 DEC 96 - 14 MARCH 97
LYNN Incorporated
D.O.E. Project - Wind River Basin
N
MSEC
1720
1680
1640
1600
1560
1520
1480
1440
1400
1360
1320
1280
1240
1200
CH1
CH2
CH3
M3a
M3b
E-A11
E-B10
D-B9
B-B14
B-B19
B-B15
A-D3
C-D7
C-D3
A-D4
B-D5
B-D8
D15
B-D19
B-D22
B-D23
E-D34
975000
970000
965000
960000
955000
950000
945000
940000
770000
775000
780000
785000
790000
795000
800000
805000
0 Ft
5000 Ft
10000 Ft
15000 Ft
20000 Ft

FIGURE 1

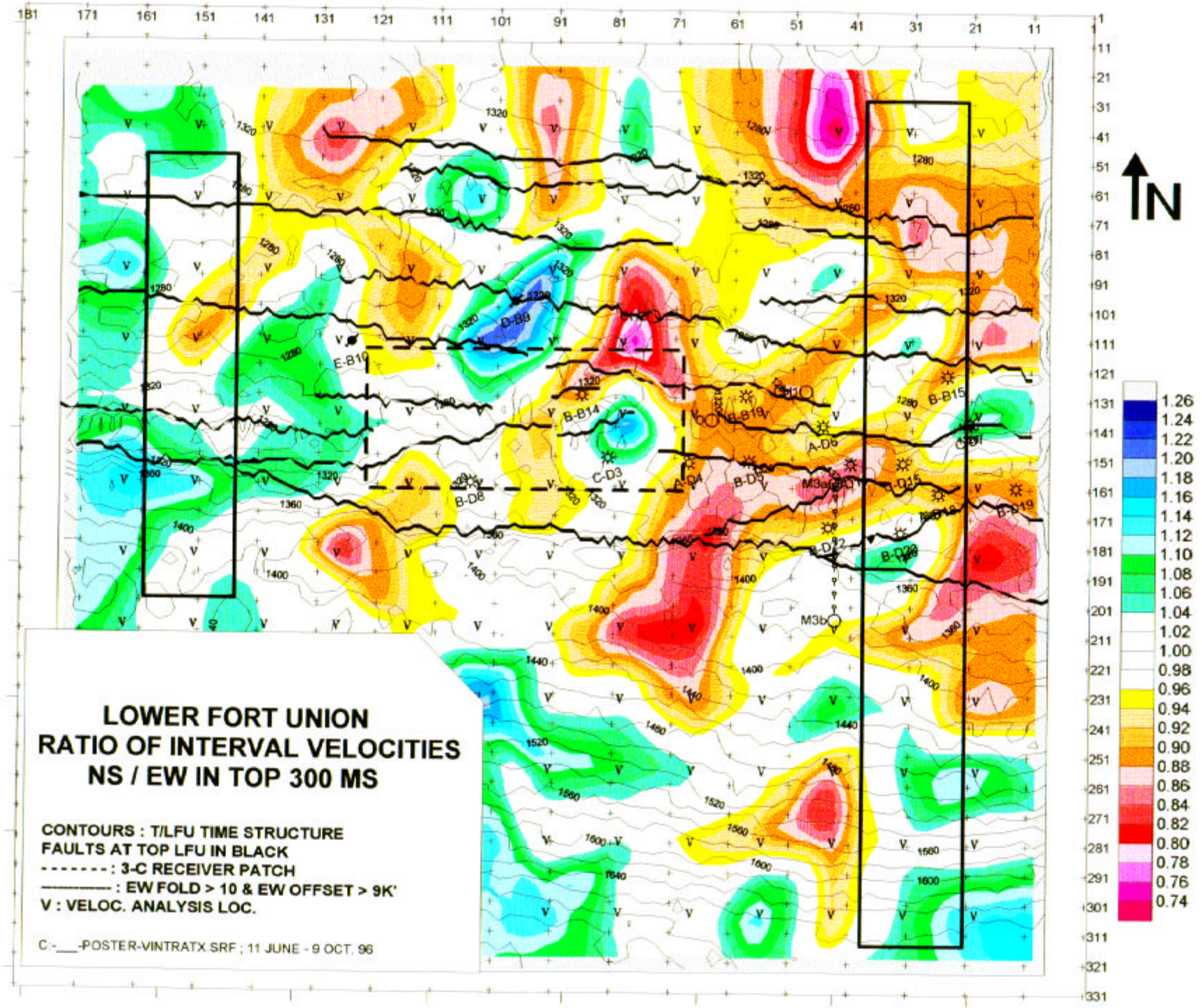

Lynn Incorporated Houston, Texas
D.O.E. Project - Wind River Basin

FIGURE 2

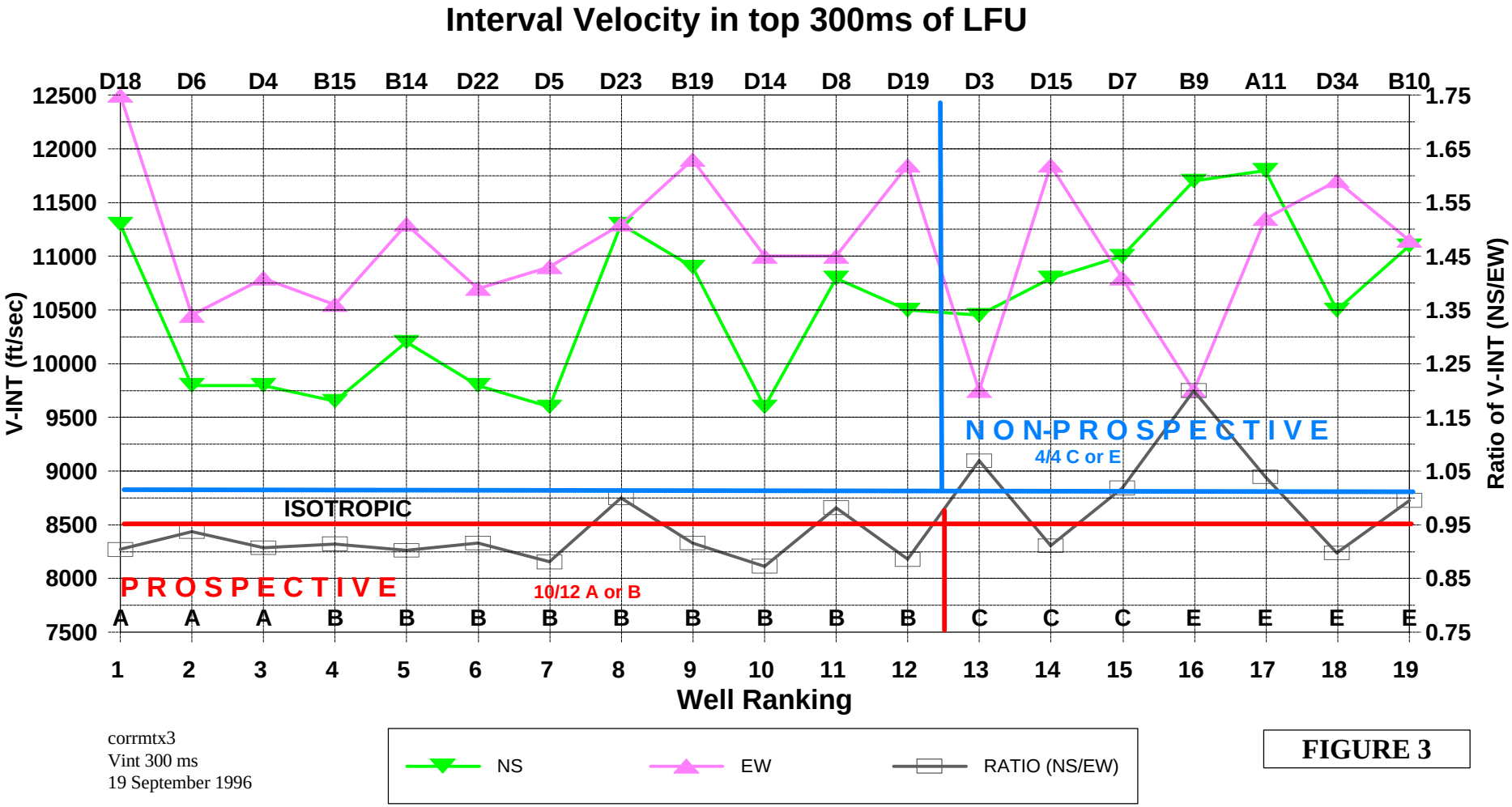

corrmtx3
Vint 300 ms
19 September 1996

FIGURE 3

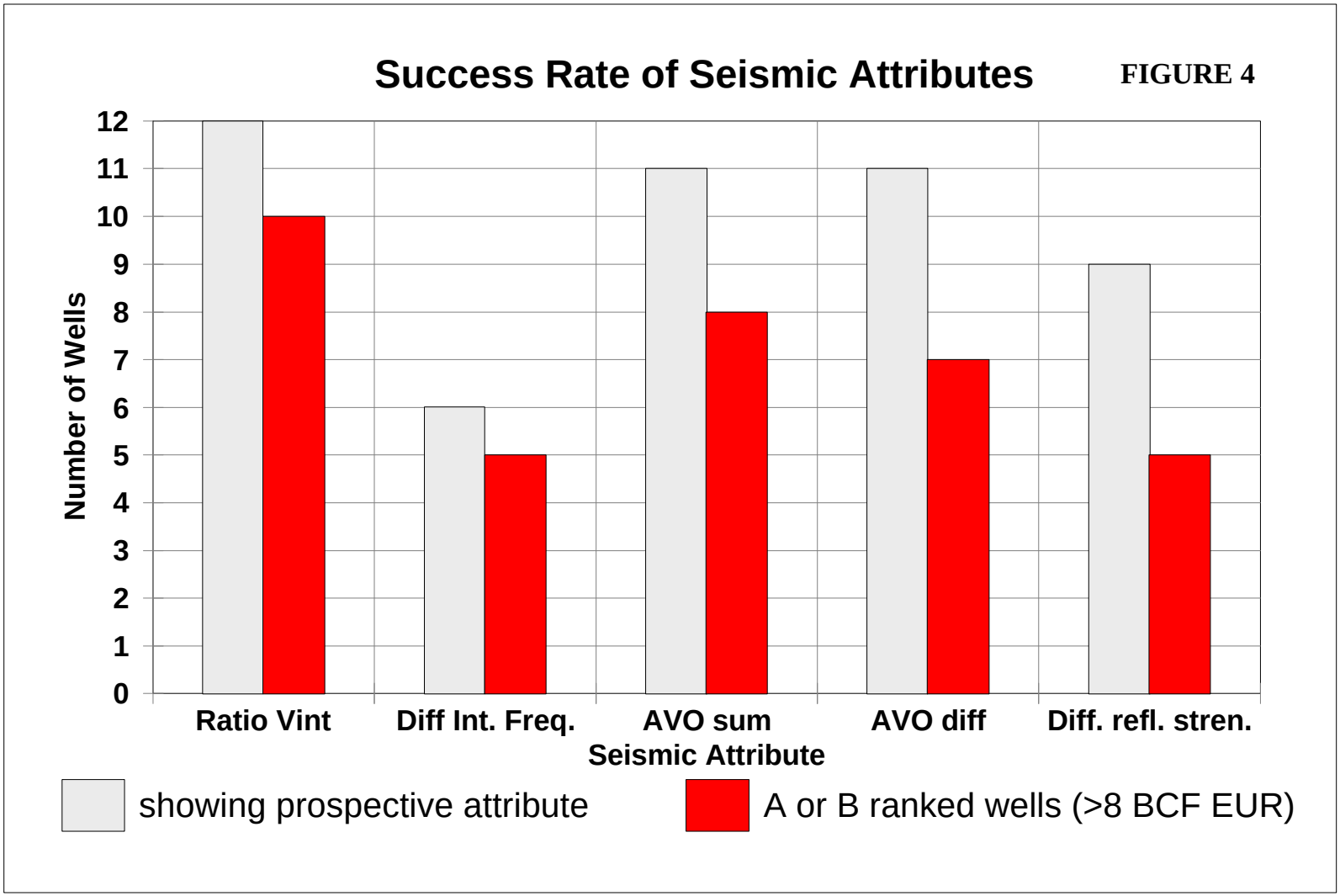
Success Rate of Seismic Attributes
FIGURE 4
Number of Wells
12
11
10
9
8
7
6
5
4
3
2
1
0
Ratio Vint
Diff Int. Freq.
AVO sum
AVO diff
Diff. refl. stren.
Seismic Attribute
showing prospective attribute
A or B ranked wells (>8 BCF EUR)

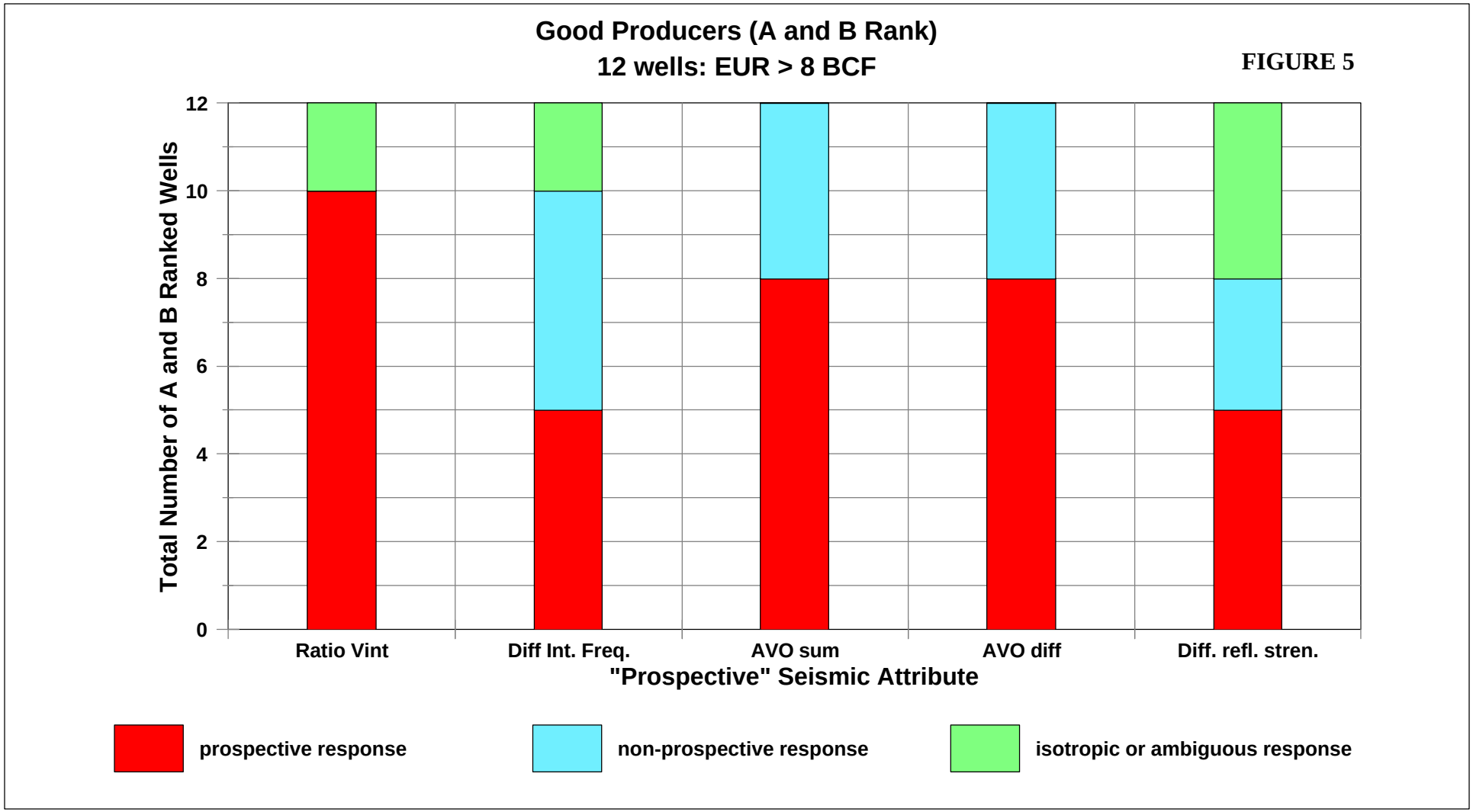
Good Producers (A and B Rank)
12 wells: EUR > 8 BCF
Total Number of A and B Ranked Wells
0
2
4
6
8
10
12
Ratio Vint
Diff Int. Freq.
AVO sum
AVO diff
Diff. refl. stren.
"Prospective" Seismic Attribute
prospective response
non-prospective response
isotropic or ambiguous response

FIGURE 5

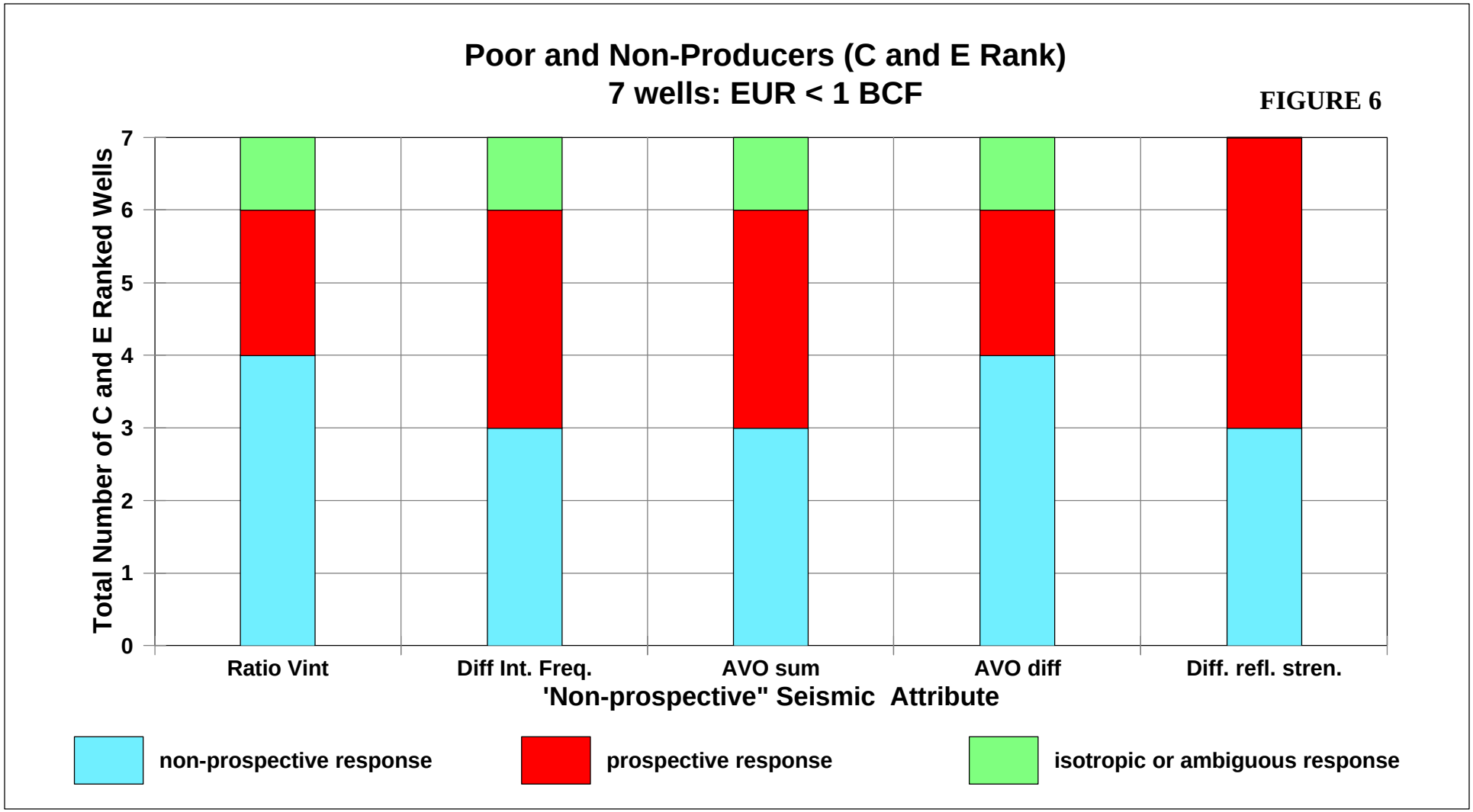
Poor and Non-Producers (C and E Rank)
7 wells: EUR < 1 BCF
FIGURE 6
Total Number of C and E Ranked Wells
0
1
2
3
4
5
6
7
Ratio Vint
Diff Int. Freq.
AVO sum
AVO diff
Diff. refl. stren.
'Non-prospective" Seismic Attribute
non-prospective response
prospective response
isotropic or ambiguous response

Z AXIS: EW TIME STRUCTURE

V : VELOCITY ANALYSIS LOCATIONS
FAULTS AT TOP LFU IN BLACK

COLOR CONTOURS:
PROSPECTIVE SEISMIC ATTRIBUTES FOR UPPER LFU (TOP 300 MS)

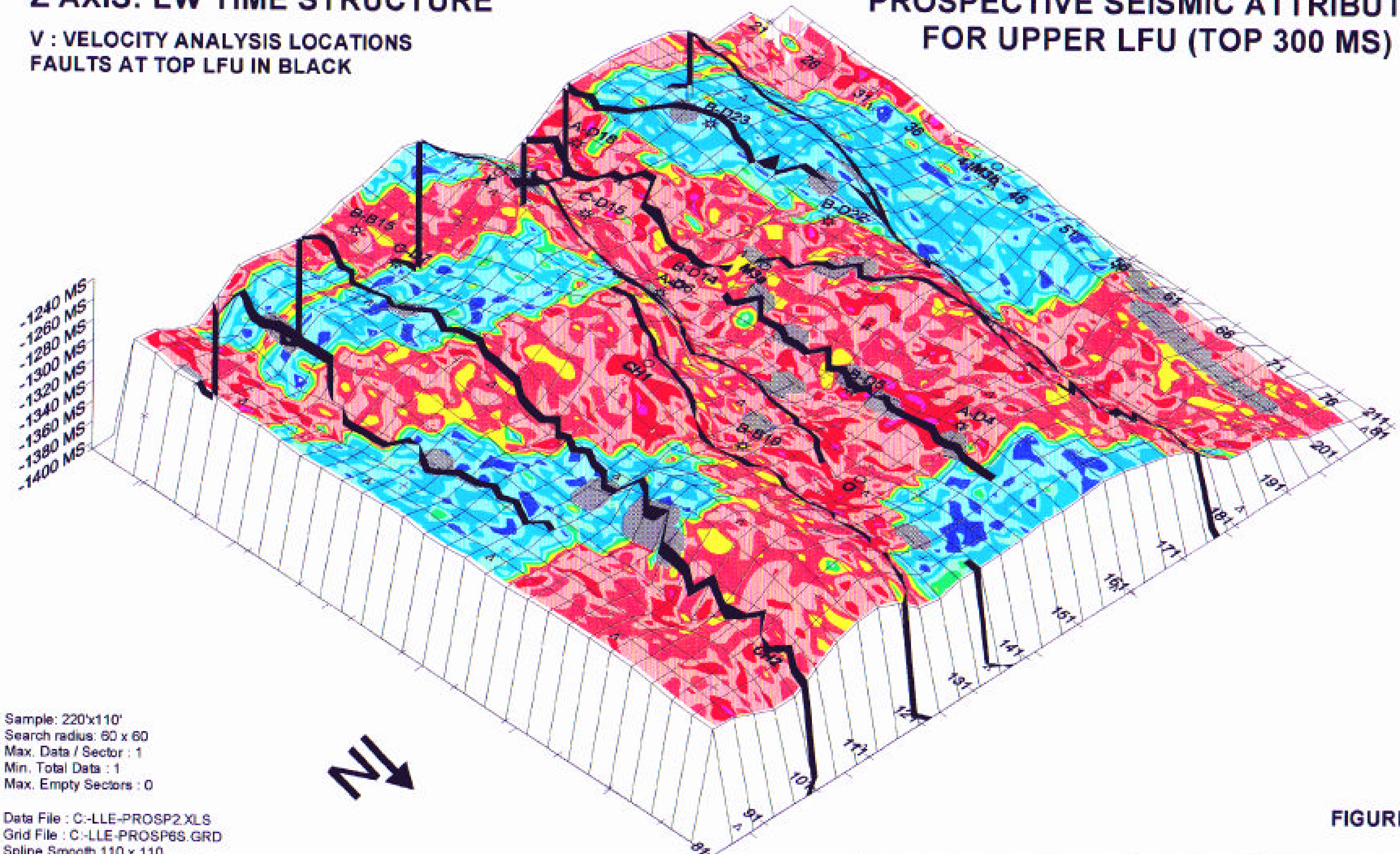

Sample: 220'x110'
Search radius: 60 x 60
Max. Data / Sector : 1
Min. Total Data : 1
Max. Empty Sectors : 0

Data File : C:-LLE-PROSP2.XLS
Grid File : C:-LLE-PROSP6S.GRD
Spline Smooth 110 x 110
Grid File Time Str. : C:-LLE-EWTIME5.GRD
X-Y Scale : 1" = 2200'
Z scale : 1" = 110'

Lynn Incorporated Houston, Texas
D.O.E. Project Wind River Basin

D:-___32-TLFU-TIMEAT3R.SRF ; 7 NOV 96 - 17 MARCH 97

FIGURE 7

0 FT 2000 FT 4000 FT 6000 FT 8000 FT

POSITIVE SEISMIC ATTRIBUTES: 0 1 2 3 4 5 6 7 8 9 NO DATA